The Microbe 8 (2025) 100448

Contents lists available at ScienceDirect

The Microbe

journal homepage: www.sciencedirect.com/journal/the-microbe

"Bleu VS Yellow": Marennine and extracellular polysaccharides for potential application in cosmetic and pharmaceutical applications

Mariame Chehouri [a], Elodie Pedron [a], Bertrand Genard [b], Kim Doiron [b], Samuel Fortin [a], William Bélanger [a], Jean-Sébastien Deschênes [c], Réjean Tremblay [a,*]

[a] Institut des Sciences de la Mer, Université du Québec à Rimouski, Rimouski, Québec, Canada
[b] Les laboratoires Iso-BioKem Inc, Rimouski, Québec, Canada
[c] Département de mathématiques, informatique et génie, Université du Québec à Rimouski, Rimouski, Québec, Canada

ARTICLE INFO

Keywords:
Haslea ostrearia
Marennine
Exopolysaccharides (EPS)
Cosmetics
Lipidomic
Dermal skin cells

ABSTRACT

Haslea ostrearia, a widely distributed marine pennate diatom, produces the unique blue pigment marennine and various extracellular polysaccharides (EPS), exhibiting promising bioactive properties. Previous studies have demonstrated the antibacterial, antioxidant, and antiproliferative effects of purified marennine extracts, while EPS fractions remain primarily understudied despite their potential applications in dermatology and cosmetics. Based on these prior findings, we hypothesized that marennine and EPS could influence skin-related biological processes, particularly gene expression related to hydration and aging, as well as lipid metabolism. To test this hypothesis, we investigated the effects of marennine and EPS at different concentrations (1, 10 and 100 μg mL^{-1}) on dermal fibroblast skin cells. Gene expression analysis targeted key markers associated with hydration and anti-aging, while lipidomic profiling assessed potential alterations in skin cell lipid composition. Our results demonstrated a significant upregulation of genes linked to skin hydration and elasticity, supporting the bioactive potential of these compounds. However, lipidomic analyses revealed no significant changes in the structural lipid composition of the skin cells across all tested concentrations. These findings highlight the potential of marennine and EPS as bioactive ingredients for cosmetic formulations aimed at improving skin hydration and anti-aging properties. Furthermore, their bioactivity suggests possible pharmaceutical applications, particularly in dermatological treatments requiring natural bioactive compounds with antioxidative and protective properties.

1. Introduction

Marennine refers to a water-soluble blue-green pigment synthesized by a benthic pennate diatom called *Haslea ostrearia* (Gastineau et al., 2014). The pigment is produced during growth and is influenced by factors like light characteristics, extended photoperiod, and potential nutrient limitation (Mouget et al., 2004). There are two distinct forms of marennine: one intracellular (IMn), which accumulates in diatom vesicles, and another extracellular (EMn), released into the culture medium (Pouvreau et al., 2006). EMn has shown diverse biological activities (see review of Gabed et al., 2022), encompassing antioxidant properties (Pouvreau et al., 2008), antiproliferative effects (Carbonelle et al., 1999; Gastineau et al., 2012), antiviral activity (Gastineau et al., 2012), antibacterial efficacy (Falaise et al., 2016) and antitumor properties (Hussein and Abdullah, 2020). EMn has exhibited promising prophylactic activity against bacteria, reducing the pathogenicity of some species and demonstrating the probiotic potential of this natural pigment (Falaise et al., 2019; Turcotte et al., 2016, Bouhlel et al., 2021). Recent research utilizing in-vivo nuclear magnetic resonance has identified that marennine at low concentration acts by stiffening bacterial membranes without affecting the bilayer's integrity and limiting the pathogenicity of Gram-negative bacteria (Bouhlel et al., 2021). Moreover, the antiproliferative activities of marennine have been documented across various human cancer cell lines, including SKOV-3 (ovarian cancer), SW116 (colon cancer), and M113 (melanoma) (Carbonelle et al., 1999; Gastineau et al., 2012). Additionally, marennine has exhibited substantial antioxidative and free radical scavenging capabilities, surpassing the efficacy of certain conventional antioxidants in the food industry, such as the flavonoid apigenin (Pouvreau et al., 2008). Furthermore, in addition to its established antioxidant and antiproliferative characteristics, Gastineau et al., (2012) provided empirical evidence supporting the antiviral efficacy of

* Corresponding author.
E-mail address: rejean_tremblay@uqar.ca (R. Tremblay).

https://doi.org/10.1016/j.microb.2025.100448
Received 16 January 2025; Received in revised form 2 July 2025; Accepted 8 July 2025
Available online 8 July 2025

marennine against the HSV-1 herpes virus. The study showed an EC50 value of 27 μg/mL, indicating marennine's potency to be twice that of the reference drug Zovirax in mitigating viral activity. Moreover, a recent study by Méresse et al., (2023) revealed that marennine exerts a time- and concentration-dependent significant impact on the dynamic alterations of neuroinflammatory processes.

EMn released by *Haslea sp.* in the culture medium culture is associated with the presence of polysaccharides (Zebiri et al.; 2023, Bélanger et al., 2025). Extracellular polysaccharides (EPS) are frequently produced by microalgae, especially diatoms (Delattre et al., 2016). These EPS play key roles in facilitating cell adhesion to surfaces or migration within biofilms, acting as a protective barrier against chemical, osmotic, and desiccation stress, while also serving as a nutrient reserve (Liu et al., 2024). EPSs are actively released by various marine organisms (Raposo et al., 2014), including *Haslea ostrearia*. In studies conducted by Bélanger et al. (2020, 2025) the identification of sulfated polysaccharides following EMn purification was observed. The research suggested that these findings hold significant scientific value emphasizing its potential importance in a broader aspect. EPSs are renowned for their anti-inflammatory, antimicrobial, and antiviral properties. These principal sugars structuring polysaccharides include xylose, glucose, mannose, and galactose (Raposo et al., 2014). Sulfated polysaccharides have been associated with blood coagulation, antilipidemic effects, and immunomodulatory properties (Bellou et al., 2014; Majtan and Jesenak, 2018). In recent years, there has been a growing trend in incorporating bioactive molecules as ingredients in cosmetic products. These bioactive molecules, also called 'actives', are distinguished by their ability to actively regulate biological processes in human skin (Goyal and Jerold, 2023).

This study aims to address these gaps by evaluating the influence of marennine and EPSs on the lipidomic profile of dermal fibroblast cells and the expression levels of targeted genes related to skin hydration, elasticity, and barrier function. By integrating gene expression and lipidomic analyses, this research provides new insights into how these natural compounds could contribute to cosmetic and pharmaceutical applications. Our findings will help bridge the existing knowledge gap and establish a scientific basis for further product development incorporating *Haslea osteria* derived bioactive. Lipidomics involves the detailed and comprehensive identification and quantification of the main molecular species of lipids. Mass spectrometry (MS)–based approaches support current lipid analysis techniques, which enable profiling of the total lipid extract from algae material without chemical modification, requiring a relatively small sample amount.

2. Materials and methods

2.1. Algal culture

Biomass production, following the methodology by Prasetiya et al. (2022), was conducted at our wet laboratory facility (Station aquicole de Pointe-aux Pères) at Université du Québec à Rimouski. *Haslea ostrearia* (strain B-48), provided by the Nantes Culture Collection, was used for algal production. The cultures were maintained semi-continuously in 30 L flat-bottomed circular Photobioreactors (PBRs) using 50 kDa ultrafiltered seawater enriched with F/2 media and supplemented with 30 mg L^{-1} of silicates. Batch cultures were grown under controlled conditions (light intensity: 180 mol photons m^{-2} s^{-1}, temperature: 20 °C, salinity: 28). Extracellular marennine, at approximately 10 mg L^{-1}, was collected after 35 days, and a 1 μm filtration process was applied to remove cellular or particulate matter. The marennine content was then quantified in the filtered culture water using a 0.22-micron syringe filter.

2.2. Marennine and Exopolysaccharide extraction

Marennine and Exopolysaccharide (EPS) samples were prepared according to the protocol described in Bélanger et al., (2025). Briefly, graphite flakes were mixed into the culture supernatant of *Haslea ostrearia* (BW) through mechanical stirring and allowed to settle. The supernatant was discarded, and the solid phase was loaded in a chromatography column for elution with an aqueous butanone solution (20 %, v/v). The raw extract was then converted into a gel by adding disodium phosphate and calcium acetate, followed by centrifugation to separate the marennine hydrogel from other EPS. The marennine fraction was washed with nanopore water (NW) and dissolved in an aqueous EDTA solution. EPS was extracted from the gelation supernatant using a rotary evaporator to dry the sample, followed by its dissolution in dilute HCl and neutralization with NaOH. The solution was then filtered on a cellulose filter, diafiltrated on a 1 kDa MWCO membrane, and freeze-dried. Finally, the extract was washed with methanol and centrifuged to preserve only the lipophobic pellet, which was freeze-dried again and dissolved in NW. As demonstrated in Bélanger et al. (2025), the marennine fraction had a molecular weight range of 3–2 kDA showing the highest level of purity reported.

2.3. Preparation, exposure, and detachment of skin cells

Primary skin cells of the dermal fibroblast type, sourced from BJ (ATCC CRL-2522) were employed in this study. These were cultured in ATCC-formulated Eagle's Minimum Essential Medium (EMEM) (Multicell, Wisent, INC). Fetal bovine serum was added to complete the growth medium, achieving a final concentration of 10 %. Triplicates of skin cell cultures were exposed or not (control) to varying concentrations of marennine and extracellular polymeric substances (EPS) after achieving cell confluence for around 3 weeks. The samples were categorized into 4 categories: control (CTRL), 1 μg mL^{-1}, 10 μg mL^{-1}, and 100 μg mL^{-1}. A minimum exposure period of 24 h was established for the cells (5×10^5 cells) across the three concentrations of marennine and EPS extract. The exposure duration was meticulously determined, considering cell growth rates, to ensure an optimal cell quantity for subsequent extractions.

After 24 h of exposure, the skin cells were prepared for detachment. Initially, the culture medium was removed, and the cells were rinsed with 5 mL of phosphate-buffered saline (PBS) (Multicell, Wisent, INC) to eliminate any residual medium. Subsequently, 10 mL of Accutase in DPBS with 0.5 mM EDTA (sterile-filtered and cell culture tested) (EMD Millipore Corp, SCR005) was added to detach the cells from the bottom of the flasks. After an incubation period of 10–15 min, cell detachment was monitored using a microscope. Once detached, the cells and Accutase solution were transferred to a 15 mL Falcon tube and centrifuged at 4000 *g* for 5 min at 20 °C. Following centrifugation, the supernatant containing Accutase was discarded, and the cell pellet was washed with 5 mL of PBS to remove any remaining Accutase. A second round of centrifugation was then performed. Finally, after discarding the PBS, the cells exposed to both marennine, and EPS were sub-sampled in two sections one for lipidomic and the second for gene expression analyses.

2.4. Cell viability

Cell viability was analyzed using the Thermo Scientific Invitrogen Countess 3 automated cell counter. A total of 12.5 μL of cells was mixed with 12.5 μL of trypan blue staining solution to achieve a 1:1 ratio. The mixture was then loaded onto Countess cell counting chamber slides to differentiate viable cells. Measurements were performed in duplicate, and the average viability was calculated.

2.5. Lipidomic analysis

Lipidomic analysis was applied on exposed skin cells with 1 mL of methyl tert-butyl ether TFE: 2,2,2 trifluoroethanol 5/1 (v/v) (MTBE/TFE) solution added to 500 μL of the cell suspension in a sonicator bath during 1 min followed by centrifugation during 5 min at 2935 rcf. MS

analysis of lipide extracts was performed with an Agilent 6546 LC-QTOF using Mass Hunter acquisition software with an Agilent Jet Stream Technology ion Source at Les laboratoires IsoBioKem (Rimouski, Qc, Canada). Q-TOF was operated at 10 GHz in high-resolution mode in a 1700 *m/z* mass range. Analysis parameters used for the lipidomic study were like those described in Koelmel et al. (2020). Briefly, the lipids extracts were chromatographically separated on an HPLC 1260 Infinity II (Agilent Technologies) using the Agilent ZORBAX Eclipse Plus C18 Rapid Resolution HD column (2.1 × 50 mm, 1.8 μm) and a C18 guard column (3.0 × 5 mm, 2.7 μm) at 50 °C. Mobile phase A was 90/10 water/methanol (v/v) containing 10 mM ammonium acetate, 0.2 mM ammonium fluoride, and 5 μM InfinityLab deactivator additive, mobile phase B was 50/30/20 isopropanol/methanol/acetonitrile (v/v/v) without ammonium acetate, 0.2 mM ammonium fluoride and 5 μM InfinityLab deactivator additive. The gradient elution used was maintained at 30 %B 0–3 min, increased to 70 % B from 3 to 5 min, increased to 86 % B 5–13 min, held at 86 %B 13–20 min, increased to 100 % B 20–21 min, maintained at 100 % B 21–27 min, and return to initial condition 27–28 min, with a flow rate at 0.35 mL min^{-1}. The total run was 30 min, followed by a 3 min post-run. The injection volumes were 2 μL for approving samples, 5 μL for negative samples, and a 15-s in-wash port for needle wash (50:50 methanol/isopropanol). Source parameters were gas temperature at 200 °C, gas flow 10 L min^{-1}, nebulizer 50 psi, sheath gas temperature at 300 °C, sheath Gas flow 12 L min^{-1}, VCap at 3000 V in negative mode and 3500 V in positive mode, nozzle voltage 0 V and fragmentor at 150 V. Reference mass ions used are: in negative mode *m/z* 112.98, 119.03, 980.01 and 1033.98 and positive mode *m/z* 121.05 and 922.00. The sample employed two data acquisition modes. First, a scan at a rate of 1 spectra s^{-1} was performed in the *m/z* range of 100–1700. Second, an iterative workflow was conducted at three collision energies 5/15/40 with three iterations by collision energy. For iteration, the MS scan was at 3 spectra s^{-1} and the MS/MS scan at 3 spectra s^{-1} in the *m/z* range of 100–1700 for both. Subsequently, lipid annotator software analysis was employed to process all data, ensuring lipid entities were well-annotated by providing structural information confidently informed by MS/MS spectra.

2.6. Quantification of gene expression

For RNA extraction, the second part of exposed skin cells was processed using the RNeasy® Micro Kit (Qiagen), strictly following the manufacturer's guidelines. Following extraction, RNA concentrations were quantified with an absorbance ratio of 260/280 using the (NanoVue Plus spectrophotometer, GE Healthcare, Pittsburgh, PA, USA). Subsequently, the RNA was reverse transcribed into cDNA for increased stability using the QuantiTect Reverse Transcription kit (50) (Qiagen). The cDNA concentration was verified via the NanoVue plus spectrophotometer, and a total concentration of 5 ng μl^{-1} was employed for calculating the total volume. Following cDNA synthesis, the quantification of gene expression was performed. The choice of target genes and the testing methodology were determined based on the modified protocol by Kong et al. (2016). Real-time reverse transcription polymerase chain reaction (RT-PCR) via Bio-Rad iCycler MyIQ PCR (thermal cycler, 19599) was conducted using the Qiagen 1 and 2 programs. The procedure involved an initial incubation period of 2 min at 42 °C, 15 min at 42 °C, and a final denaturation step of 3 min at 95 °C. Custom-designed primers and probes specific to the genes listed in Table 1 were employed for this analysis.

In this study, the housekeeping gene 36B4 served as the reference standard for evaluating the expression of various target genes. Each gene was systematically compared with the housekeeping gene (36B4), and subsequently, the Fold Change (log^2) was computed for every sample dose (1 μg mL^{-1}, 10 μg mL^{-1},100 μg mL^{-1}) represented as (M1, M10, M100 and EPS1, EPS10, EPS100) for each targeted gene. As a result, a threshold amplification value of 1 was assigned where values surpassing it denoted overexpression, while those below indicated under expression. The mean (n = 3), standard deviation (STDV), and standard error (SE) were then calculated.

Quantitative PCR (qPCR) analyses were performed using a comparative Ct method. The procedure consisted of two stages: an initial

Table 1
Primer design for targeted genes with forward and reverse sequences (5′–3′).

Targeted genes	Primer names	Usage	Forward Sequence (5′–3′)	Reverse Sequence (5′–3′)
Housekeeping	36B4	**Reference gene**	ATGCAGCAGATCCGCATGT	TGCGCATCATGGTGTTCTT
Cellular retinoic acid-binding protein II	CRABPII	**Skin Hydration Products**	CAAGACCTCGTGGACCAGAGA	ACCCTGGTGCACACAACGT
Ceramide synthase 4	LASS4		GTTTCAACGAGTGGTTTTG	TGAATCTCTCAAAGGCAAG
Fibrillin-1	FBN1		CCCTGGGATTTACCGTGCTT	CTGCCCGTTGTTCTGGATCT
Aquaporin	AQP3		TCAAAGACCTGTGGAACTGGTATC	TGATGGTGAGGAAACCACCG
Collagen Type I	COL1A1	**Anti-aging products**	GATTCCCTGGACCTAAAGGTGC	AGCCTCTCCATCTTTGCCAGCA
Collagen Type III	COL3A1		TGGTCTGCAAGGAATGCCTGGA	TCTTTCCCTGGGACACCATCAG
Corneodesmosin	CDSN	**Whitening products**	TCTGGTTCCAGGCATGACCTAC	GCTGGAGAAGTATTTGCCCTCAG
Acetyl-Coenzyme-A carboxylase 1	ACACA	**Slimming products**	CCCAGATTCTGCGTTTAAGA	CATCCACAATGTAAGCACCA
Human 3-hydroxy-3-methylglutaryl-Co-enzyme A reductase	HMGCR		GACGTGAACCTATGCTGGTCAG	GGTATCTGTTTCAGCCACTAAGG
Thioredoxin	TRX	**Oxidative stress and antioxidants**	GACAAGAGAAAGAAGTGAAAAGATAAA	TGGACCCCTTTATTGAAACGTT
Copper-zinc-superoxide dismutase	CuZnSOD		ATGATCTCATTGGATCTTCACG	CTCCTGAAAAGAGAGCTGCAC
Glutathione peroxidase 1	GPX		TTCCCGTGCAACCAGGTTT	AGGGAATTCAGAATCTCTTCGTT
Dynamin 1 like	DRP1	**Immune response-inflammation**	GGACGCTAATTCCTGTCATAA	CAGGCTTTCTAGCACTGAGC
Interleukin 1 beta	IL-1B		TTCTTCGACACATGGGATAAC	TCCCGGAGCGTGCAGTTCA
Interleukin 6	IL6		GATGGATGCTTCCAATCTGGAT	AGGTACTCTAGGTATACCTCAAACTCCAA
Tumor protein p53	P53		CTGGCACGGAACAGCTTTGA	CCTTTCTTGCGGAGATTCTCTTC
ERCC excision repair 1, endonuclease non-catalytic subunit	ERCC	**Cell repair**	GAAATTTGTGATACCCCTCGAC	GATCGGAATAAGGGCTTGG
Hypoxanthine phosphoribosyl transferase	HPRT		GCTATAAATTCTTTGCTGACCTGCTG	AATTACTTTTATGTCCCCTGTTGACTGG
Matrix metallopeptidase 1	MMP1		GGGAGATCATCGGGACAACTC	AATACCTGGGCCTGGTTGAAA
Mitochondrial nucleoid factor 1	MNF1	**Mitochondrial integrity**	ATATGGAAGACGTACGCAGAC	CCCCTGTGCTTTTTGCTTTC
OPA1 Mitochondrial dynamin like GTPase	OPA1		GGCTCCTGACACAAAGGAAA	TCCTTCCATGAGGGTCCATT
Cellular Communication Network Factor 1	CCN1		TCAAAGACCTGTGGAACTGGTATC	CACAAATCCGGGTTTCTTTCA
Glucuronidase beta	GUSB	**Skin structure**	TGCAGGTGATGGAAGAAGTG	TTGCTCACAAAGGTCACAGG
Periaxin	PRX		CAGGCTTGATGGTATCACTGC	AGGCCTTCCAGTTCACTGAC

denaturation stage at 95 °C for 20 s, followed by an annealing and extension stage at 60 °C for an additional 20 s. Notably, a melting stage was omitted. These reactions were conducted through 40 cycles and were carried out in triplicate. The reactions were executed in MicroAmp™ Fast Optical 96-Well Reaction Plates with a 0.1 mL volume, employing Fast SYBR™ Green Master Mix from Applied Biosystems. The qPCR assays were validated using the QuantStudio™ 3 System Real-time PCR platform from Thermo Fisher.

2.7. Statistical analysis

Cell viability was analyzed by one-way ANOVA analysis performed following validation of assumptions was met, normality distribution by Shapiro-Wilk test and homoscedasticity by the Ben-Levene test on XLSTAT for both marennine and EPS tested at four concentrations (CTRL, 1 μg mL^{-1}, 10 μg mL^{-1}, and 100 μg mL^{-1}).

MetaboAnalyst version 6.0, an advanced web-based analytical platform for high-throughput visualization of lipidomic data, was utilized for both univariate and multivariate statistical analyses of lipidomics and gene expression data. Principal component analysis (PCA) was conducted on autoscaled data. Statistically significant differences among the examined groups of concentrations of marennine and EPS (CTRL, 1 μg mL^{-1}, 10 μg mL^{-1}, and 100 μg mL^{-1}) were evaluated using a one-way ANOVA test, with a threshold of $p < 0.05$ denoting statistical significance. Where differences were detected, Tukey's multiple multiple comparison tests were used to determine which means were significantly different.

3. Results

3.1. Cell viability

ANOVA results demonstrated no significant difference between both extracts at all three concentrations and the control, with a P-value of 0.458, degrees of freedom (DF) = 6, and F = 1.008.

3.2. Lipidomic analysis

LC-QTOF results identified 191 lipid classes in skin cells exposed to EPS and marennine. Among these, 32 lipid classes were significant for marennine exposure (Table 2) compared to 44 classes for EPS (Table 3), as determined by the ANOVA test. Subsequent analyses focused on these significant classes. The Principal Component Analysis (PCA) for skin cells exposed to EPS, as shown in Fig. 1(a), produced a 2-D score plot containing two distinct clusters of samples. These clusters were separated along PC1, which accounts for 46.9 % of the total variance. Notably, there was an overlapping of ellipses for EPS1 and EPS10, with a partial separation of the EPS1 cluster. The Variable Importance in Projection (VIP) score plot shown in Fig. 1(b), highlighted the 6 highest classes having a VIP score higher than 1.8, primarily related to the phosphatidylcholine (PC) class. Specifically, PC 35:1 was predominantly associated with the control (CTRL) group, whereas PC 32:1:16:0, PC 31:0, PC 38:4, PC 34:2, and phosphatidylethanolamine (PE) 38:5 was more associated with EPS 100. For marennine, the PCA shown in Fig. 1 (c) indicated heterogeneity in the lipid classes across all concentrations. The ellipses for the three marennine concentrations overlapped with PC1 explaining 64.8 % of the variance. The VIP score plot in Fig. 1(d), identified six lipid classes with VIP scores exceeding 2.3, mainly within the PC class. Specifically, PC 32:1 was significantly associated with M10, like PC 34:2 and ether-linked PC 33:6. Meanwhile, PC 30:0 14:0 was associated with M10, PC 36:2 was more significant for M100, and sphingomyelin (SM) M1 predominantly explained 34:1.

3.3. Quantification of gene expression

In this study, 27 targeted genes, each with different roles in skin products, were analyzed. Results obtained using real-time qPCR identified the gene expression profiles in skin cells exposed to EPS and marennine. Among these 27 genes, 7 showed significant expression changes for marennine exposure (Table 4), while 17 genes were substantial for EPS (Table 5), as determined by the ANOVA test. Genes were considered upregulated when expression fold-change values were greater than 2.

The Principal Component Analysis (PCA) results for skin cells exposed to EPS, depicted in Fig. 2(a), produced a 2-D score plot demonstrating two distinct sample clusters. These clusters were separated along PC1, which accounts for 72.9 % of the total variance. Notably, there was a significant distance between the ellipse for EPS100 and those for EPS1 and EPS10, which exhibit overlapping ellipses. As for marennine shown in Fig. 2(b), we noticed the clusters were separated along PC1, which accounts for 53.5 % of the total variance. Remarkably, we observed an important distance between the ellipse for M1 and M100. In the evaluation of marennine concentrations within this study, data for M10 was excluded due to missing information. As illustrated in Fig. 3(a) through the Variable Importance in Projection (VIP) score plot, the four most significant gene classes with VIP scores exceeding 1.5 were Prx, FBN1, HMGCR, and MMP1, which were primarily associated with skin structure, skin hydration, slimming, and cell repair products, respectively. The fold change regulation presented in Fig. 3(b) further elucidates these findings. Specifically, for skin hydration, Fibrillin-1 (FBN1) exhibited significant upregulation at 100 μg mL^{-1}, standing out as the only gene in this category with notable expression. In the anti-aging category, Collagen Type III (COL3A1) showed upregulation at 100 μg mL^{-1}. Among the genes associated with skin-whitening products, Corneodesmosin (CDSN) showed no amplification. For the slimming category, Human 3-Hydroxy-3-Methylglutaryl-Coenzyme A Reductase (HMGCR) demonstrated substantial amplification at 100 μL. Within the oxidative stress and antioxidant category, both Thioredoxin (Trx) and Glutathione Peroxidase 1 (GPX) displayed significant

Table 2
ANOVA test results of the significant lipid classes for skin cells exposed to marennine.

Name	P-value
EtherPC 33:6	5.9302e − 08
TG 72:9	8.7347e − 05
TG 73:9	0.000
MG 24:1	0.000
MG 25:1	0.001
TG 22:1	0.001
DHSph 16:0	0.001
LPC 14:0	0.001
EtherPE 23:3	0.001
PS 34:1	0.001
LPC 16:1	0.001
MG 23:1	0.001
TG 48:0	0.001
EtherLPE 16:0	0.002
PI 76:19	0.002
TG 55:1	0.002
LPC 17:0	0.002
TG 54:1	0.002
LPC 16:0	0.002
EtherLPC 16:0	0.004
EtherPE 40:5	0.004
LPC 20:4	0.005
EtherPE 40:7	0.005
LPC 18:1	0.005
EtherPE 38:6	0.005
DG 36:0	0.006
TG 48:2	0.007
Cer_NS 34:2	0.007
PC 36:3	0.007
EtherPE 40:10	0.007
TG 30:2	0.007
PC 32:0	0.008

Table 3
ANOVA test results of the significant lipid classes for skin cells exposed to EPS.

Name	P-value
PC 38:2	0.000
PC 30:1	0.000
EtherPE 40:7	0.000
PS 34:1	0.000
PC 34:4	0.000
PE 38:4	0.000
PC 36:6	0.000
PI 38:4	0.000
PE 38:5	0.000
MG 25:1	0.000
EtherPE 42:11	0.000
PS 36:1	0.001
PC 35:1	0.001
EtherLPE 16:0	0.001
EtherPE 40:10	0.001
MG 24:1	0.001
PE 36:4	0.001
PC 35:3	0.002
PC 30:1|PC 12:0_18:1	0.002
PC 37:4	0.002
LPC 16:1	0.002
EtherPE 40:5	0.002
PC 32:0|PC 27:0_5:0	0.003
PE 36:2	0.003
TG 49:9	0.003
TG 73:9	0.004
PC 40:7	0.004
PS 38:4	0.004
LPC 14:0	0.004
PC 30:0|PC 14:0_16:0	0.004
PC 32:2|PC 16:1_16:1	0.004
PC 38:3	0.005
PC 36:5|PC 16:1_20:4	0.005
EtherPC 35:8	0.006
TG 48:1	0.006
EtherPE 36:4	0.006
TG 57:2	0.007
TG 48:2	0.008
PC 29:0	0.008
PC 34:2	0.008
EtherPE 40:6	0.008
PE 40:7	0.010
PS 40:6	0.010
TG 56:1	0.010

amplification at concentrations of 1 μg mL^{-1} and 10 μg mL^{-1}. The immune response-inflammation category revealed downregulation of Dynamin 1 (DRP1), Interleukin 1 Beta (IL-1B), and Tumor Protein p53 (P53), while Interleukin 6 (IL-6) was notably upregulated at 100 μg mL^{-1}. In terms of cell repair, ERCC excision repair 1, endonuclease non-catalytic subunit (ERCC) was upregulated at both tested concentrations, and Mitochondrial Nucleoid Factor (MMP1) showed upregulation at 1 μg mL^{-1}. For mitochondrial integrity, Mitochondrial Dynamin-Like GTPase (OPA1) was upregulated at 1 μg mL^{-1}. Finally, no genes within the skin structure category exhibited significant amplification. These findings underscore the varied gene expression profiles elicited by different marennine concentrations, highlighting the specific genes that were significantly modulated.

ANOVA analysis identified 17 significant genes within skin cells exposed to EPS, as illustrated in Fig. 3(c) using the Variable Importance in Projection (VIP) score plot. Notably, the four most significant classes with VIP scores exceeding 1.5 are FBN1, ACACA, COL1A1, and IL-1B, which were primarily associated with skin hydration, slimming, anti-aging, and immune response-inflammation products, respectively. Additionally, the analysis of EPS gene expression, depicted in Fig. 3(d), revealed that among genes pertinent to skin hydration, only Fibrillin-1 (FBN1) showed significant upregulation at a concentration of 100 μg mL^{-1}. In the anti-aging category, Collagen Type I (COL1A1) exhibited significant amplification at 1 μg mL^{-1}, while Collagen Type III (COL3A1) showed over expression at 10 μg mL^{-1}. As for the gene associated with skin-whitening products, Corneodesmosin (CDSN) showed no amplification. For slimming products, Acetyl-Coenzyme A Carboxylase 1 (ACACA) and Human 3-Hydroxy-3-Methylglutaryl-Coenzyme A Reductase (HMGCR) manifested significant amplification at 10 μg mL^{-1}. Within the oxidative stress and antioxidant domain, Thioredoxin (Trx) and Glutathione Peroxidase 1 (GPX) showed minimal amplification across all concentrations. In contrast, Copper-Zinc-Superoxide Dismutase (CuZnSOD) demonstrated upregulation at 10 μg mL^{-1}. In the immune response-inflammation category, Interleukin 1 Beta (IL-1B) exhibited significant amplification at 100 μg mL^{-1}. Tumor Protein p53 (P53) showed minimal amplification at 10 μg mL^{-1}, while Interleukin 6 (IL-6) and Dynamin 1 (DRP1) showed no gene expression. No significant gene amplification was detected in the cell repair category. For mitochondrial integrity, Mitochondrial Nucleoid Factor 1 (MNF1) and OPA1 Mitochondrial Dynamin-Like GTPase (OPA1) displayed minimal amplification (below 2) at 10 μg mL^{-1}. Conversely, no gene amplification was observed among the targeted genes in the skin structure category.

4. Discussion

4.1. Lipidomic analysis

Lipidomic results showed no significant change in the lipid classes of skin cells exposed to both marennine and EPS, as indicated by the PCA results, which showed no distance between ellipses for both EPS (1 μg mL^{-1}, and 10 μg mL^{-1}) and marennine (1 μg mL^{-1}, 10 μg mL^{-1}, 100 μg mL^{-1}) treatments. Note that EPS 100 μg mL^{-1} was lost. Based on these findings, we suggest that neither marennine nor EPS induces skin structure or composition changes. This can be considered a positive outcome, as it indicates that incorporating marennine or EPS in whatever concentrations into cosmetic creams does not cause any adverse impact on the skin. In contrast, other research has shown different results for microalgae extract exposed to dermal skin cells. For instance, Łuczaj et al. (2023), studied the impact of *Nannochloropsis oceanica* lipid extract on the phospholipid profile of human keratinocytes subjected to UVB radiation. The outcomes revealed that treating keratinocytes with the lipid extract from microalgae reduced sphingomyelin (SM) levels, with a more pronounced effect observed in UVB-irradiated cells. At the same time, there was a notable increase in ceramides CER[NDS] and CER[NS], as well as heightened sphingomyelinase activity. Moreover, the rise in alkylacylPE (PEo) and diacylPE (PE) species content seen in UVB-exposed keratinocytes after being treated with the microalgal extract indicated a possible activation of pro-survival pathways.

The most prevalent lipid class in skin cells was phosphatidylcholine (PC), which, along with phosphatidylglycerol (PG), phosphatidylethanolamine (PE), phosphatidylinositol (PI), phosphatidic acid (PA), and phosphatidylserine (PS), belongs to the glycerophosphate lipids. These lipids serve as essential cell signaling molecules and components of the plasma membrane, contributing significantly to its integrity and stability. Phospholipids and ceramides are the primary lipid fractions found in skin cells (Knox and O'Boyle, 2021). They function as structural components of the cell membrane, affecting its permeability, and play a vital role in cell signaling (D'Orazio et al., 2013). Research indicates that among these lipids, PC and PE have specific roles in decreasing lipofuscin levels in cuticle cells, with PC demonstrating a more pronounced effect (Cui et al., 2018).

Phosphatidylcholine (PC) is notable for its intrinsic hydration force and metabolites that act as essential osmoprotectants in skin cells. Hydrogenated phosphatidylcholine (HPC), composed of saturated fatty acids, shares physical properties with components of the skin permeability barrier. PC and HPC and their metabolites demonstrate preventive efficacy against pathological states caused by redox imbalance and free radical generation. This property is advantageous in drug

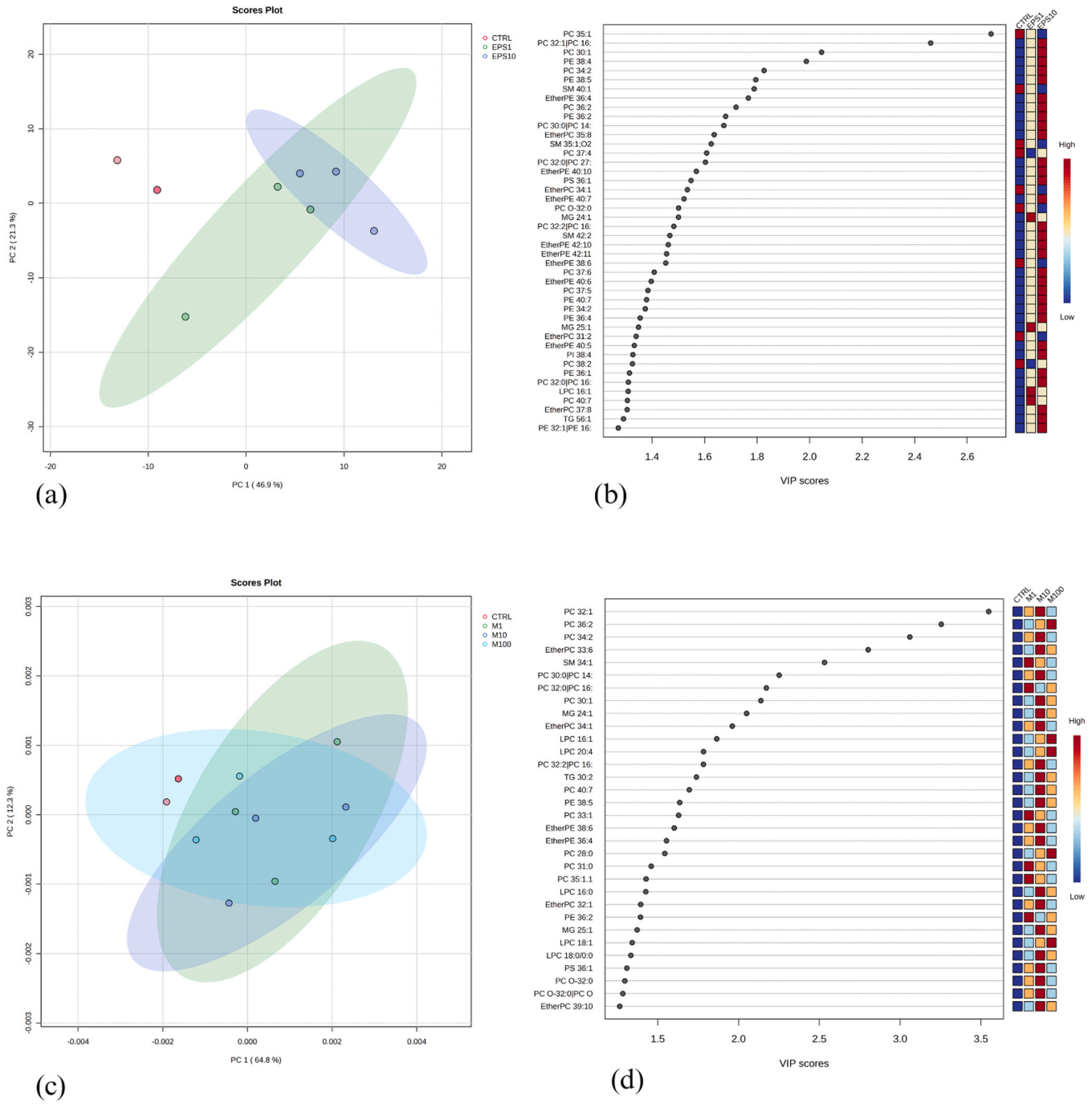

Fig. 1. Multivariate data analysis of lipidomic for positive ions for both marennine and EPS. A principal Component Analysis (PCA) scores plots (left panels), Variable Importance in Projection (VIP) (right panels). (a) Principal Component Analysis (PCA) score plot for EPS (EPS1, EPS10). (b) VIP score plot of the top lipid classes exposed to EPS (EPS1, EPS10). (c) Principal Component Analysis (PCA) score plot for marennine (M1, M10, M100). (d) VIP score plot of the top lipid classes exposed to marennine (M1, M10, M100).

Table 4
ANOVA test results of the significant targeted genes exposed to marennine.

Name	P-value	FDR
ACACA	0.037	0.042
AQUA	0.029	0.001
CuZnSOD	0.043	0.001
DRP1	0.039	0.001
GUSB	0.034	0.002
HPRT	0.038	0.002
PRX	0.038	0.002

formulations, where PC helps mitigate certain drug side effects (Ghyczy and Vladimir, 2002).

One limitation of our study is that only a limited set of lipid species were analyzed, and potential changes in minor lipid subclasses may not have been detected. Additionally, while our study focused on fibroblasts, future research should explore the effects of marennine and EPS on keratinocytes and other skin cell types to obtain a more comprehensive understanding of their bioactivity. Further investigations using in vivo models could provide valuable insights into long-term effects and optimal formulation strategies.

Table 5
ANOVA test results of the significant targeted genes exposed to EPS.

Name	P-value
FBN1	0.000
ERCC	0.000
CRABPII	0.000
CCN1	0.000
GUSB	0.000
AQUA	0.000
PRX	0.000
P53	0.001
ACACA	0.001
CuZnSOD	0.003
GPX	0.004
IL6	0.004
HMGCR	0.005
OPA1	0.008
COL3A	0.015
MNF1	0.026
HPRT	0.035

4.2. *Quantification of gene expression*

This study investigated the effects of the bioactive molecules marennine and EPS on primary dermal fibroblast-type skin cells. Our findings revealed that marennine increases gene expression in primary cells, specifically targeting Trx, FBN1, HMGCR, and GPX. Regarding EPS our results showed an upregulation in targeting genes like FBN1, ACACA, COL1A1, and IL_1B genes. The FBN1 gene is identified as encoding fibrillin-1, a significant extracellular matrix glycoprotein integral to the structural framework of 10–12 nm calcium-binding microfibrils. These microfibrils are essential architectural elements within the upper dermis, forming part of the dermal elastic fiber network that supports the integrity and functionality of all connective tissues (Sakai et al., 2016; Watson et al., 1999). The ACACA gene was shown to encode a multifunctional enzyme system critical for fatty acid synthesis (Bhattacharjee et al., 2020). As the HMGCR gene also functions as the pivotal enzyme that catalyzes the rate-limiting step in the de novo synthesis of cholesterol in the liver, specifically transforming HMG-CoA into mevalonate, both ACACA, and HMGCR are genes responsible for slimming and reducing fatty acids (Dong et al., 2024). The genes Trx and GPX, belong to the cellular antioxidant systems. Thioredoxin (Trx) and glutathione peroxidase (GPX) systems play a crucial role in reducing oxidative stress. These antioxidant defense mechanisms are essential for maintaining an optimal redox balance in melanocytes by neutralizing reactive oxygen species (ROS). This protective function helps guard against oxidative stress, excessive melanogenesis, and photo-damaged skin (Lu et al., 2021). Additionally, the COL1A1 gene, which provides instructions for synthesizing type I collagen, was highlighted. Type I collagen is the most prevalent collagen form in the human body and is crucial for the structural support of various tissues, including cartilage, bone, tendons, and skin (Li et al., 2022). Furthermore, the IL1B gene, responsible for encoding interleukin-1 beta (IL-1β), plays a pivotal role in the body's inflammatory response. IL-1β is involved in inducing fever and promoting the production of additional proinflammatory cytokines, underscoring its significance in immune response and inflammation (Yin et al., 2023).

Our findings align with those of Han et al. (2024), who investigated mRNA expression levels and wound healing effects in human skin cells and assessed the skin improvement effects of EPS derived from *P. cruentum*. They proposed a mechanism for skin condition improvement by integrating individual skincare mechanisms of six genes such as aquaporin 3, filaggrin, involucrin, loricrin, elastin, and fibrillin-1. Likewise, they discovered that the exopolysaccharides from P. cruentum increased the expression of genes linked to skin hydration, barrier strengthening, and elasticity, and facilitated wound healing by promoting fibroblast migration. Another study by Letsiou et al. (2017) found that *Nannochloropsis gaditana* extract possesses significant in vitro skin protection activity against induced oxidative stress, highlighting its potential to protect skin from oxidative stress. Results of this study agree with the statement as upregulation of the CuZnSOD gene responsible for oxidative stress was observed. Regarding the upregulation of the COL1A1 gene, a similar trend was observed by Toucheteau et al. (2023), who investigated the effect of six different microalgae EPS extracts on fibroblast skin cells. They examined both native and depolymerized forms of EPS. They observed that the depolymerized forms exhibited significantly higher pro-collagen activity, increasing collagen

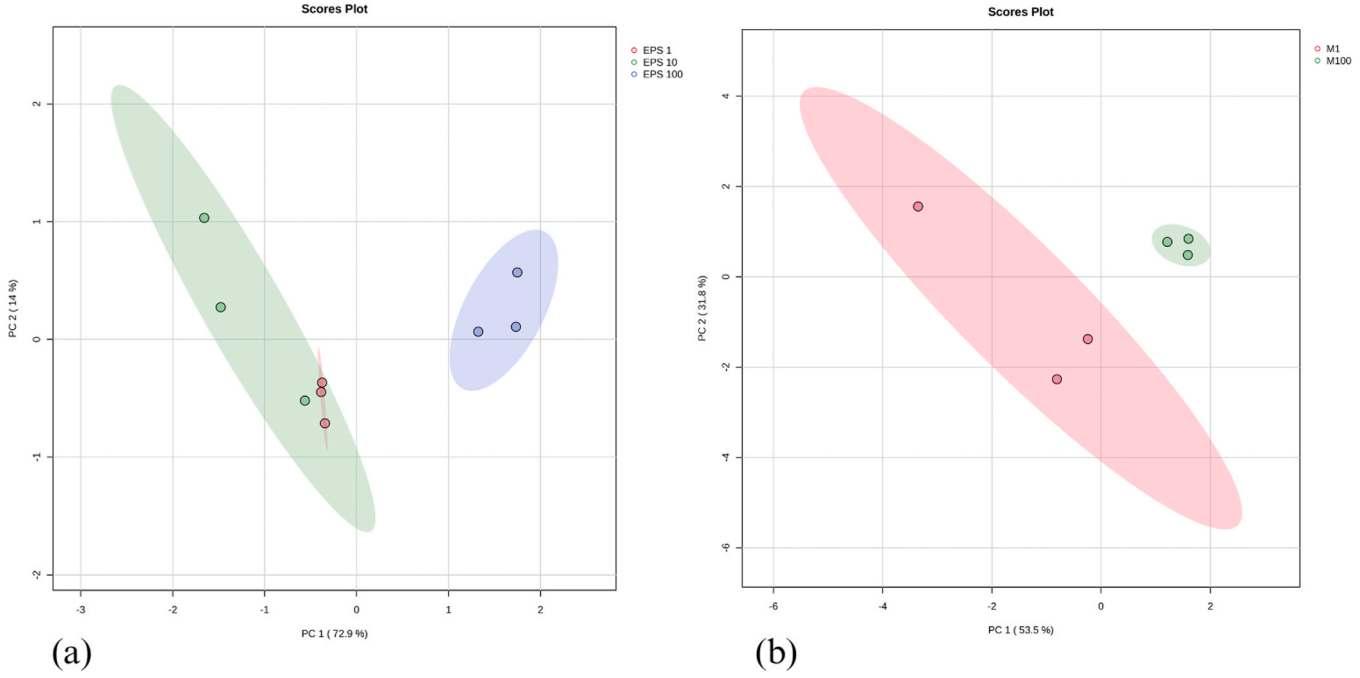

Fig. 2. Multivariate data analysis of gene expression for both marennine and EPS. (a) Principal Component Analysis (PCA) score plots for EPS. (b) Principal Component Analysis (PCA) score plots for marennine.

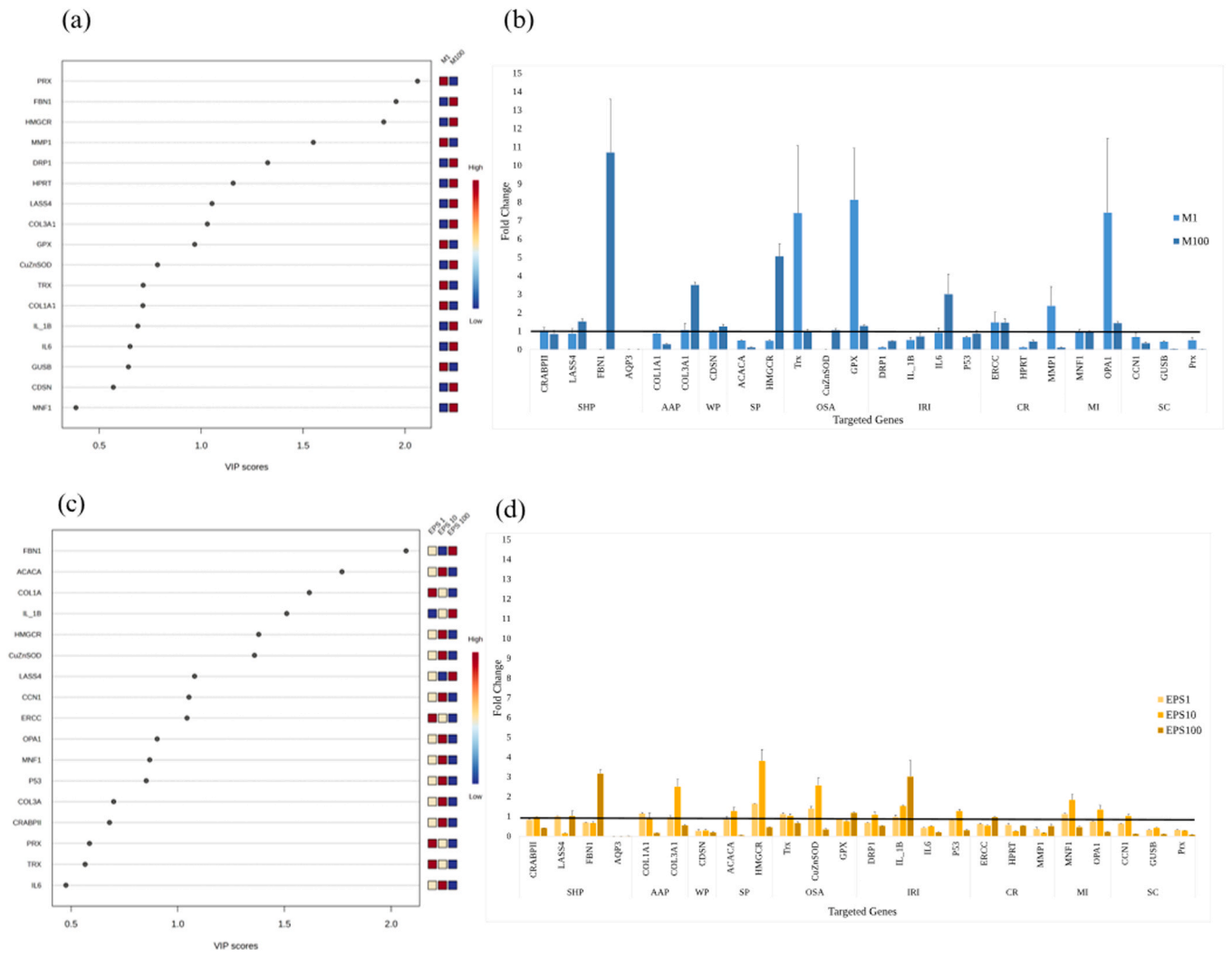

Fig. 3. (a) Variable importance in projection (VIP) of top 17 genes for Marennine. (b) Fold change of DNA expression in targeted genes for Marennine. (c) Variable Importance in Projection (VIP) of top 17 genes for EPS. (d) Fold change of DNA expression in targeted genes for EPS. Categories from left to right: SHP (Skin hydration products), AAP (Anti-aging products), WP (Whitening products), SP (Slimming products), OSA (Oxidative stress and antioxidants), IRI (Immune response-inflammation), CR (Cell repair), MI (Mitochondrial integrity), and SC (Skin structure).

production by at least 100 % for the less active forms and over 300 % for the most active forms. For instance, collagen production was enhanced by approximately 394 %, 388 %, and 326 % by the RFB-Dep forms of EPS from *D. ennorea*, *Glossomastyx sp.*, and *P. tricornutum*, respectively. They also noted that microalgae EPS could inhibit up to 27 % of human matrix metalloproteinase-1 (MMP-1) activity, consistent with our findings of downregulating the MMP1 gene. Similarly, Abdolbaghian et al. (2021) study found that *C. vulgaris* extract on fibroblast skin cells increased the gene expression of type I collagen supporting our results. Furthermore, our results showed an expression of genes responsible for antioxidant activities, aligning with the findings of Lu et al. (2021). They found that *Chlorella minutissima* extract exhibited high inhibitory potency towards tyrosinase and elastase, suggesting a potential role in controlling skin aging, inflammatory processes, and pigmentation. Additionally, the impact of *C. minutissima* extract on a human hepatoma cell line (Huh-7) was evaluated to analyze the expression of genes (SOD1, GPx1, GPx2) involved in the oxidative stress response. The results indicated the absence of cytotoxic effects from the aqueous extracts. Specifically, SOD1 and GPx1 expression levels were slightly upregulated and downregulated, respectively, while GPx4 expression remained unaffected.

PCA results on EPS and marennine extracts indicated a noticeable difference between concentrations, particularly with 100 μg mL^{-1} for both extracts showing a visible distance between ellipses. This can be interpreted as 100 μg mL^{-1} being a high concentration, potentially unsuitable for use in creams. Additionally, 100 μg mL^{-1} is a concentration of marennine or EPS requiring a significant amount of biomass, reducing its economic potential. Therefore, using 10 μg mL^{-1} or 1 μg mL^{-1} as optimal concentrations can be more cost-effective and sustainable. Our findings in genomics revealed that the most upregulated genes for both marennine and EPS were those targeting hydration. Interestingly, our lipidomic results showed an abundance of PC, further suggesting that these extracts positively affect the skin barrier through their hydration properties.

The ability of marennine and EPS to modulate gene expression without significantly altering lipid composition is particularly relevant for skincare applications. Hydration and anti-aging benefits are key targets in cosmetic formulations, and bioactive compounds that enhance these functions without disrupting membrane integrity are highly desirable. Additionally, the antioxidative and protective properties of marennine, previously documented in antimicrobial and antiviral studies (Falaise et al., 2016; Gastineau et al., 2012), suggest potential applications in dermatological treatments, particularly for conditions linked to oxidative stress and inflammation.

For large-scale industrial applications, stabilizing marennine and EPS is a critical consideration, as bioactive compounds can degrade due to environmental factors such as light, temperature, and oxidation. Encapsulation techniques, such as lipid-based nanocarriers, microencapsulation with biopolymers, or lyophilization, have been successfully used in the cosmetic and pharmaceutical industries to enhance the stability and bioavailability of natural extracts (Lohcharoenkal et al., 2014). Additionally, incorporating these bioactives into emulsions with antioxidant stabilizers could further prevent degradation and improve formulation longevity in creams, serums, or pharmaceutical ointments.

5. Conclusion

In summary, this study provides new insights into the beneficial role of *Haslea ostrearia* bioactive compounds in the domain of cosmetics. Marennine and exopolysaccharides (EPS) demonstrate promising potential in cosmetic formulations, being rich in ingredients that offer hydration, anti-aging benefits, and antioxidant properties. Additionally, these compounds are efficient without altering the skin's lipid composition, as evidenced by an elevated amount of phosphatidylcholine (PC) in skin cells. Our findings also present a new understanding of the optimal concentrations of both extracts for use in cosmetics. While 100 μg mL^{-1} produced significant differences, 1 and 10 μg mL^{-1} yielded promising results, suggesting that these lower concentrations are both effective and more economical. This study broadens our understanding of how marennine and EPS can be utilized in cosmetic applications, providing valuable guidelines for their effective and sustainable use.

CRediT authorship contribution statement

Samuel Fortin: Writing – review & editing, Supervision, Methodology, Data curation. **Kim Doiron:** Writing – review & editing, Supervision, Methodology, Formal analysis, Data curation. **Bertrand Genard:** Writing – review & editing, Validation, Supervision, Methodology, Investigation, Funding acquisition, Formal analysis, Data curation, Conceptualization. **Elodie Pedron:** Writing – review & editing, Validation, Methodology, Formal analysis. **Mariame Chehouri:** Writing – review & editing, Writing – original draft, Visualization, Validation, Software, Methodology, Formal analysis, Data curation, Conceptualization. **Tremblay Rejean:** Writing – review & editing, Validation, Supervision, Project administration, Methodology, Investigation, Funding acquisition, Formal analysis, Conceptualization. **Jean-Sébastien Deschênes:** Writing – review & editing, Supervision, Funding acquisition, Conceptualization. **William Bélanger:** Writing – review & editing, Methodology.

Declaration of Competing Interest

The authors declare that they have no known competing financial interests or personal relationships that could have appeared to influence the work reported in this paper.

Acknowledgments

We want to express our sincere gratitude to all those who have contributed to the successful completion of this research. Firstly, we thank Nathalie Gauthier for microalgae production and the research team at Iso-Biokem for their collaboration, insightful discussions, and technical assistance. We also appreciate the financial support from MITACS (No. FRB3111) Ministère de l'Économie et de l'Innovation du Québec (No. PADS-56972) and Ressources Aquatiques Québec, Research network funded by Fonds de Recherche du Québec Nature et Technologies (No. 2020-RS4-265329).

Data availability

Data will be made available on request.

References

Abdolbaghian, S., Jamili, S., Manayi, A., Mashinchian Moradi, A., 2021. Chlorella growth factor extraction and its effect on gene expression of types I and III collagen in skin fibroblast cells cells. Iran. J. Fish. Sci. 20 (6), 1664–1673. https://doi.org/10.22092/ijfs.2021.125435.

Bélanger, W., Arnold, A.A., Turcotte, F., Saint-Louis, R., Deschênes, J.S., Genard, B., Marcotte, I., Tremblay, R., 2020. Extraction improvement of the bioactive blue-green pigment "marennine" from diatom *Haslea ostrearia's* blue water: a solid-phase method based on graphitic matrices. Mar. Drugs 18, 653. https://doi.org/10.3390/md18120653.

Bélanger, W., Saint-Louis, R., Genard, B., Deschênes, J.-S., Tremblay, R., 2025. Scalable purification of marennine and other exopolymers from diatom *Haslea ostrearia's* "blue water". Algal Res. 86, 103879. https://doi.org/10.1016/j.algal.2024.103879.

Bellou, S., Baeshen, M.N., Elazzazy, A.M., Aggeli, D., Sayegh, F., Aggelis, G., 2014. Microalgal lipids biochemistry and biotechnological perspectives. Biotech. Adv. 32 (8), 1476–1493. https://doi.org/10.1016/j.biotechadv.2014.10.003.

Bhattacharjee, K., Nath, M., Choudhury, Y., 2020. Fatty acid synthesis and cancer: aberrant expression of the ACACA and ACACB genes increases the risk for cancer. Meta Gene 26, 100798. https://doi.org/10.1016/j.mgene.2020.100798.

Bouhlel, Z., Arnold, A.A., Deschênes, J.S., Mouget, J.L., Warschawski, D.E., Tremblay, R., Marcotte, I., 2021. Investigating the action of the microalgal pigment marennine on *Vibrio splendidus* by in vivo 2H and 31P solid-state NMR. Biochim. Biophys. Acta Biomembr. 1863 (9), 183642. https://doi.org/10.1016/j.bbamem.2021.183642.

Carbonelle, Delphine, Pondaven, Philippe, Morançais, Michèle, Masse, Guillaume, Bosh, Steffi, Jacquot, Cyril, Briand, Glen, Robert, Jean-Michel, Roussakis, Christos, 1999. Antitumor and antiproliferative effects of an aqueous extract from the marine diatom *Haslea ostrearia* (Simonsen) against solid tumors: lung carcinoma (NSCLC-N6), kidney carcinoma (E39) and melanoma (M96) cell lines. Anticancer Res. 19 (1A), 621–624.

Cui, L., He, C. fen, Fan, L., Jia, Y., 2018. Application of lipidomics to reveal differences in facial skin surface lipids between males and females. J. Cosmet. Dermatol. 17 (6), 1254–1261. https://doi.org/10.1111/jocd.12474.

Delattre, C., Pierre, G., Laroche, C., Michaud, P., 2016. Production, extraction and characterization of microalgal and cyanobacterial exopolysaccharides. Biotech. Adv. 34 (7), 1159–1179. https://doi.org/10.1016/j.biotechadv.2016.08.001.

Dong, J., Li, M., Peng, R., Zhang, Y., Qiao, Z., Sun, N., 2024. ACACA reduces lipid accumulation through dual regulation of lipid metabolism and mitochondrial function via AMPK-PPARα-CPT1A axis. J. Transl. Med. 22, 196. https://doi.org/10.1186/s12967-024-04942-0.

D'Orazio, J., Jarrett, S., Amaro-Ortiz, A., Scott, T., 2013. UV radiation and the skin. Int. J. Mol. Sci. 14 (6), 12222–12248. https://doi.org/10.3390/ijms140612222.

Falaise, C., François, C., Travers, M.A., Morga, B., Haure, J., Tremblay, R., Turcotte, F., Pasetto, P., Gastineau, R., Hardivillier, Y., Leignel, V., Mouget, J.L., 2016. Antimicrobial compounds from eukaryotic microalgae against human pathogens and diseases in aquaculture. Mar. Drugs 14 (9), 159. https://doi.org/10.3390/md14090159.

Falaise, C., James, A., Travers, M.A., Zanella, M., Badawi, M., Mouget, J.L., 2019. Complex relationships between the blue pigment marennine and marine bacteria of the genus *Vibrio*. Mar. Drugs 17 (3), 160. https://doi.org/10.3390/md17030160.

Gabed, N., Verret, F., Peticca, A., Kryvoruchko, I., Gastineau, R., Bosson, O., Séveno, J., Davidovich, O., Davidovich, N., Andrzej, W., Kristoffersen, J.B., Benali, A., Ioannou, E., Koutsaviti, A., Roussis, V., Gâteau, H., Phimmaha, S., Leignel, V., Badawi, M., Mouget, J.-L., 2022. What was old is new again: the pennate diatom Haslea ostrearia (Gaillon) Simonsen in the multi-omic age. Mar. Drugs 20, 234. https://doi.org/10.3390/md20040234.

Gastineau, R., Pouvreau, J.B., Hellio, C., Morançais, M., Fleurence, J., Gaudin, P., Bourgougnon, N., Mouget, J.L., 2012. Biological activities of purified marennine, the blue pigment responsible for the greening of oysters. J. Agric. Food Chem. 60 (14), 3599–3605. https://doi.org/10.1021/jf205004.

Gastineau, R., Turcotte, F., Pouvreau, J.B., Morançais, M., Fleurence, J., Windarto, E., Prasetiya, F.S., Arsad, S., Jaouen, P., Babin, M., Coiffard, L., Couteau, C., Bardeau, J. F., Jacquette, B., Leignel, V., Hardivillier, Y., Marcotte, I., Bourgougnon, N., Tremblay, R., Deschênes, J.-S., Badawy, H., Paseto, Davidovich, N., Hansen, G., Dittmer, J., Mouget, J.-L., 2014. Marennine, promising blue pigments from a widespread *Haslea* diatom species complex. Mar. Drugs 12 (6), 3161–3189. https://doi.org/10.3390/md12063161.

Ghyczy, M., Vladimir, V., 2002. Phosphatidylcholine and skin hydration. In: Leyden, J.J., Rqwlings, A.V. (Eds.), Skin Moisturization. CRC Press, Boca Raton, pp. 302–322.

Goyal, N., Jerold, F., 2023. Biocosmetics: technological advances and future outlook. Environ. Sci. Pollut. Res. 30 (10), 25148–25169. https://doi.org/10.1007/s11356-021-17567-3.

Han, S.-I., Heo, Y.M., Jeon, M.S., Kyung, S., Kang, S., Kwon, S.-J., Ryu, J.H., Kim, J.H., Ahn, J.-W., 2024. The effect of exopolysaccharides from EMS-induced *Porphyridium cruentum* mutant on human epidermal and dermal layers. Front. Mar. Sci. 11, 1365311. https://doi.org/10.3389/fmars.2024.1365311.

Hussein, H.A., Abdullah, M.A., 2020. Anticancer compounds derived from marine diatoms. Mar. Drugs 18 (7). https://doi.org/10.3390/md18070356 (MDPI AG.

Knox, S., O'Boyle, N.M., 2021. Skin lipids in health and disease: A review. Chem. Phys. Lipids 236, 105055. https://doi.org/10.1016/j.chemphyslip.2021.105055.

Koelmel, J., Sartain, M., Salcedo, J., Murali, A., Li, X., Stow, S., 2020. Improving Coverage of the Plasma Lipidome Using Iterative MS/MS Data Acquisition Combined with Lipid Annotator Software and 6546 LC/Q-TOF. Application note, Lipidomics, Agilent, 10p.

Kong, R., Cui, Y., Fisher, G.J., Wang, X., Chen, Y., Schneider, L.M., Majmudar, G., 2016. A comparative study of the effects of retinol and retinoic acid on histological, molecular, and clinical properties of human skin. J. Cosmet. Dermatol. 15 (1), 49–57. https://doi.org/10.1111/jocd.12193.

Letsiou, S., Kalliampakou, K., Gardikis, K., Mantecon, L., Infante, C., Chatzikonstantinou, M., Labrou, N.E., Flemetakis, E., 2017. Skin protective effects of *Nannochloropsis gaditana* extract on H2O2-stressed human dermal fibroblasts. Front. Mar. Sci. 4, 221. https://doi.org/10.3389/fmars.2017.00221.

Li, X., Sun, X., Kan, C., Chen, B., Qu, N., Hou, N., Liu, Y., Han, F., 2022. COL1A1: a novel oncogenic gene and therapeutic target in malignancies. Pathol. Res. Pract. 236, 154013. https://doi.org/10.1016/j.prp.2022.154013.

Liu, X., Zou, L., Li, B., Di Martino, P., Rittschof, D., Yang, J.-L., Maki, J., Liu, W., Gu, J.-D., 2024. Chemical signaling in biofilm-mediated biofouling. Nat. Chem. Biol. 20, 1406–1419. https://doi.org/10.1038/s41589-024-01740-z.

Lohcharoenkal, W., Wang, L., Chen, Y.C., Rojanasakul, Y., 2014. Protein nanoparticles as drug delivery carriers for cancer therapy. BioMed Res. Int. 2 (2014), 180549. https://doi.org/10.1155/2014/180549.

Lu, Y., Tonissen, K.F., Di Trapani, G., 2021. Modulating skin colour: role of the thioredoxin and glutathione systems in regulating melanogenesis. Biosci. Rep. 41 (5). https://doi.org/10.1042/BSR20210427.

Łuczaj, W., Gęgotek, A., Conde, T., Domingues, M.R., Domingues, P., Skrzydlewska, E., 2023. Lipidomic assessment of the impact of *Nannochloropsis* oceanica microalga lipid extract on human skin keratinocytes exposed to chronic UVB radiation. Sci. Rep. 13, 22302. https://doi.org/10.1038/s41598-023-49827-2.

Majtan, J., Jesenak, M., 2018. β-Glucans: multi-functional modulator of wound healing. Molecules 23 (4), 806. https://doi.org/10.3390/molecules23040806.

Méresse, S., Gateau, H., Tirnan, T., Larrigaldie, V., Casse, N., Pasetto, P., Mouget, J.L., Mortaud, S., Fodil, M., 2023. *Haslea ostrearia* pigment marennine affects key actors of neuroinflammation and decreases cell migration in murine neuroglial cell model. Int. J. Mol. Sci. 24 (6), 5388. https://doi.org/10.3390/ijms24065388.

Mouget, J.L., Rosa, P., Tremblin, G., 2004. Acclimation of *Haslea ostrearia* to light of different spectral qualities – confirmation of "chromatic adaptation" in diatoms. J. Photochem. Photobiol. B Biol. 75 (1–2), 1–11. https://doi.org/10.1016/j.jphotobiol.2004.04.002.

Pouvreau, J.B., Morançais, M., Fleury, F., Rosa, P., Thion, L., Cahingt, B., Zal, F., Fleurence, J., Pondaven, P., 2006. Preliminary characterisation of the blue-green pigment " marennine" from the marine tychopelagic diatom *Haslea ostrearia* (Gaillon/Bory) Simonsen. J. Appl. Phycol. 18 (6), 757–767. https://doi.org/10.1007/s10811-006-9087-x.

Pouvreau, J.B., Morançais, M., Taran, F., Rosa, P., Dufossé, L., Guérard, F., Pin, S., Fleurence, J., Pondaven, P., 2008. Antioxidant and free radical scavenging properties of marennine, a blue-green polyphenols pigment from the diatom *Haslea ostrearia* (Gaillon/Bory) Simonsen responsible for the natural greening of cultured oysters. J. Agric. Food Chem. 56 (15), 6278–6286. https://doi.org/10.1021/jf073187.

Prasetiya, F.S., Foret, M., Deschênes, J.S., Gastineau, R., Mouget, J.L., Tremblay, R., 2022. Semi-continuous system for benthic diatom cultivation and marennine production. Algal Res. 62, 102633. https://doi.org/10.1016/j.algal.2022.102633.

Raposo, M.F.D.J., De Morais, A.M.M.B., De Morais, R.M.S.C., 2014. Influence of sulphate on the composition and antibacterial and antiviral properties of the exopolysaccharide from *Porphyridium cruentum*. Life Sci. 101 (1–2), 56–63. https://doi.org/10.1016/j.lfs.2014.02.013.

Sakai, L.Y., Keene, D.R., Renard, M., De Backer, J., 2016. FBN1: the disease-causing gene for Marfan syndrome and other genetic disorders. Gene 592 (1), 279–291. https://doi.org/10.1016/j.gene.2016.07.033.

Toucheteau, C., Deffains, V., Gaignard, C., Rihouey, C., Laroche, C., Pierre, G., Lépine, O., Probert, I., Le Cerf, D., Michaud, P., Arnaudin-Fruitier, I., Bridiau, N., Maugard, T., 2023. Role of some structural features in EPS from microalgae stimulating collagen production by human dermal fibroblasts. Bioengineered 14, 2254027. https://doi.org/10.1080/21655979.2023.2254027.

Turcotte, F., Mouget, J.L., Genard, B., Lemarchand, K., Deschênes, J.S., Tremblay, R., 2016. Prophylactic effect of *Haslea ostrearia* culture supernatant containing the pigment marennine to stabilize bivalve hatchery production. Aquat. Living Res. 29 (4), 401. https://doi.org/10.1051/alr/2016032.

Watson, R.E., Griffiths, C.E., Craven, N.M., Shuttleworth, C.A., Kielty, C.M., 1999. Fibrillin-rich microfibrils are reduced in photoaged skin. Distribution at the dermal-epidermal junction. J. Invest. Dermatol. 112 (5), 782–787. https://doi.org/10.1046/j.1523-1747.1999.00562.x.

Yin, J., Wang, C., Vogel, U., Ma, Y., Zhang, Y., Wang, H., Sun, Z., Du, S., 2023. Common variants of pro-inflammatory gene IL1B and interactions with PPP1R13L and POLR1G in relation to lung cancer among Northeast Chinese. Sci. Rep. 13, 7352. https://doi.org/10.1038/s41598-023-34069-z.

Zebiri, I., Jacquette, B., Francezon, N., Herbaut, M., Latigui, A., Bricaud, S., Tremblay, R., Pasetto, P., Mouget, J.-L., Dittmer, J., 2023. The polysaccharidic nature of the skeleton of marennine as determined by NMR spectroscopy. Mar. Drugs 21, 42. https://doi.org/10.3390/md21010042.